AN EFFICIENT COLOR IMAGE QUALITY METRIC
WITH LOCAL-TUNED-GLOBAL MODEL

Ke Gu, Guangtao Zhai, Xiaokang Yang, and Wenjun Zhang

Insti. of Image Commu. & Infor. Proce., Shanghai Jiao Tong Univ., Shanghai, China, 200240
Shanghai Key Laboratory of Digital Media Processing and Transmissions
E-mail: gukesjtuee@sjtu.edu.cn

ABSTRACT

This paper investigates the problem of full-reference (FR) image quality assessment (IQA). In general, the ideal IQA metric should be effective and efficient, yet most of existing FR IQA methods cannot reach these two targets simultaneously. Under the supposition that the human visual perception to image quality depends on salient local distortion and global quality degradation, we introduce a novel effective and efficient local-tuned-global (LTG) model induced IQA metric. Extensive experiments are conducted on five publicly available subject-rated color image quality databases, including LIVE, TID2008, CSIQ, IVC and TID2013, to evaluate and compare our algorithm with classical and state-of-the-art FR IQA approaches. The proposed LTG is shown to work fast and outperform those competing methods.

Index Terms— Image quality assessment (IQA), full-reference (FR), local-tuned-global (LTG), image gradient

1. INTRODUCTION

Image quality assessment (IQA) is an important topic in digital image processing due to its applicable instruction and optimization for image/video compression [1]-[3], restoration [4], and denoising [5]-[6]. In particular, the IQA research is in the stage of highly booming evolution in recent years. On the one hand, many studies were devoted to the subjective IQA by recording real human ratings under the condition of specific image distortion types, viewing environments and inexperienced viewers. Several famous subject-rated image quality databases are LIVE [7], TID2008 [8], CSIQ [9], and IVC [10]. Very lately, Ponomarenko *et al.* released the TID2013 [11], which is up to now the largest image quality database consisting of totally 3000 distorted images. It is easy to find the subjective assessment is usually a time-consuming, laborious and costly task, and this makes it in most cases serve as the testing tool for the objective assessment.

Hundreds of objective IQA metrics [12]-[27], on the other hand, have been developed so far, to automatically predict the image quality via a variety of strategies, for instance, perceptual model, natural scene statistics, saliency detection,

machine learning, and brain science. In this paper, we concentrate on FR IQA models, which assume that the original and distorted images are entirely known. Mean-squared error (MSE) and its equivalent peak signal-to-noise ratio (P-SNR) are a couple of frequently used quality measures for images, on account of their simple definitions and clear physical meanings. Nevertheless, MSE and PSNR do not take the relevance of neighboring image pixels into account, leading them to poorly correlating with the human judgement of image quality, i.e. mean opinion score (MOS) [28]. Some classical IQA approaches [12]-[15] were therefore proposed mainly depending on structural information or statistic information. They were found to have a high consistency with subjective quality ratings for the commonly encountered natural distortion categories, such as JPEG/JPEG2000 compression, Gaussian blur and white noise.

Those classical IQA metrics, however, work ineffectively for other distortion types, e.g. quantization noise. To this end, these years has witnessed the emergence of a flood of methods with more robust performance for various kinds of distortion types. For example, feature similarity index (FSIM) [20] and gradient similarity index (GSIM) [21] were designed based on the fact that the human visual system (HVS) primarily perceives a visual signal with low-level features, and internal generative mechanism (IGM) [22] operates with the segmentation of an input image into predicted and disorderly areas followed by the integration of modified PSNR and SSIM values that are calculated on those two areas with psychophysical parameters provided in [13].

Notwithstanding the prosperity of existing FR IQA algorithms, few of them can overcome the drawback of hardly simultaneously achieving effective (high prediction accuracy) and efficient (low computational complexity) goals. In this paper, we suppose that the HVS tends to combine sensations of salient local artifacts and global quality degradation to yield the overall prediction score. Under this supposition, we first extract image gradient magnitude (GM) since it is highly sensitive to image distortions. We then independently use the local and global average poolings to estimate the local and global HVS perceptions, followed by fusing them to generate
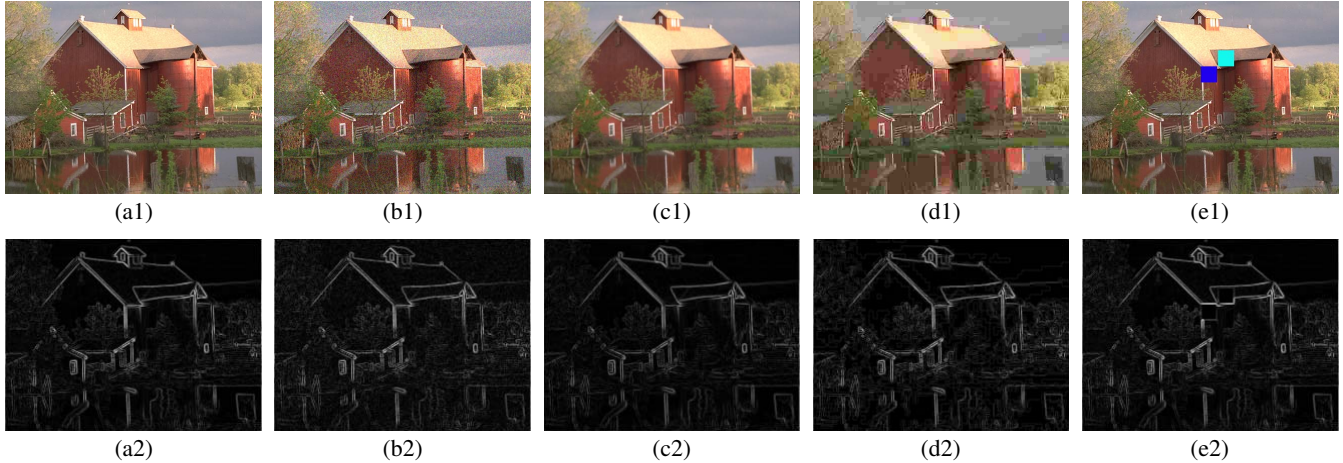
Fig. 1. Examples of representative images from TID2013 [11] and the associated image gradient maps: (a1) original image; (b1) white noise; (c1) Gaussian blur; (d1) JPEG compression; (e1) local block-wise distortions of different intensity; (a2)-(e2) gradient maps of (a1)-(e1).

the image quality score. In addition, the influence of chrominance information on IQA performance is also considered, and thus we employ the simple and widely used YIQ color space [29] to convert the RGB color image before the computation of the GM. Following those above steps, this paper develops an effective and efficient local-tuned-global (LTG) model inspired IQA algorithm.

The rest of this paper is arranged as follows. Section 2 first introduces the proposed LTG algorithm in detail. Section 3 compares our technique with classical and state-of-the-art IQA approaches in prediction performance and implementation speed, and presents experimental results to prove the superiority of the LTG method. We finally conclude the whole paper in Section 4.

2. LOCAL-TUNED-GLOBAL MODEL INSPIRED IQA METRIC

The HVS is strongly sensitive to the GM in a visual signal, which has been widely used in many applications of image processing and computer vision, such as object extraction, optical flow, and image segmentation. In recent years, the GM is also found to be very useful in IQA measures [20]-[22], and this motivates us to first extract gradient information from an input image. In this paper, we adopt the Scharr operator [30], which is essentially expressed by convolution masks as shown in Fig. 2. The GM is given by

$$G = \sqrt{G_h^2 + G_v^2} \qquad (1)$$

where G_h and G_v are the partial derivatives of the input image along horizontal and vertical directions using the Scharr operator. We display an original image and its distorted versions of 'white noise', 'Gaussian blur', 'JPEG compression' and 'local block-wise distortions of different intensity' in Fig. 1(a1)-(e1), and the associated GM maps in Fig. 1(a2)-(e2).

$$\frac{1}{16}\begin{bmatrix} 3 & 0 & -3 \\ 10 & 0 & -10 \\ 3 & 0 & -3 \end{bmatrix} \qquad \frac{1}{16}\begin{bmatrix} 3 & 10 & 3 \\ 0 & 0 & 0 \\ -3 & -10 & -3 \end{bmatrix}$$

(a) horizontal direction   (b) vertical direction

Fig. 2. Scharr gradient operator [30].

We then adopt the frequently employed similarity measure, which has three merits of symmetry, boundedness and unique maximum [12], to detect the difference of GM maps of the original image **x** and its contaminated version **y**:

$$G_m(\mathbf{x}, \mathbf{y}) = \frac{2G_x \cdot G_y + C_1}{G_x^2 + G_y^2 + C_1} \qquad (2)$$

where G_x and G_y indicate the GM of the original and distorted images, and C_1 is a positive constant for stability. Fig. 3 shows $1-G_m$ of Fig. 1(b1)-(e1), where the brighter gray level means the lower similarity, and thus higher distortion level. We can find that G_m succeeds to capture the remarkable distinction between the original and distorted images.

It is natural to use the simplest global average pooling after the distortion map is detected, as defined as follows:

$$G_g(\mathbf{x}, \mathbf{y}) = \Phi(G_m) = \frac{1}{M}\sum_{i=1}^{M} G_m(x_i, y_i) \qquad (3)$$

where M is the total number of pixels in the image, and Φ computes the mean value. Note that Fig. 1(a1) is the original image, and Fig. 1(b1)-(e1) indicate contaminated versions which have similar MOS values, as listed in Table 1. We calculate the G_g values of those distorted images, and tabulate them in Table 1. It is very clear that G_g gives different prediction scores for those four distorted images. In particular, the G_g value of 'local block-wise distortions of different intensity' corrupted image is noticeably different from others.

Table 1. Predictions of various IQA metrics for Fig. 1(b1)-(e1).

	MOS	SSIM	VIF	FSIM	G_g	G_l
Fig. 1(b1)	3.7180	0.7951	0.3769	0.9194	0.9900	0.9992
Fig. 1(c1)	3.7838	0.9334	0.5101	0.9568	0.9954	0.9997
Fig. 1(d1)	3.5897	0.8202	0.2309	0.9027	0.9897	0.9991
Fig. 1(e1)	3.7368	0.9845	0.9697	0.9825	0.9976	0.9999

We also use three representative IQA metrics that use global average pooling, including SSIM, VIF and FSIM, to predict those four distorted images, and report the results in Table 1. Similarly, these three methods encounter the same trouble.

We believe this shortage of the global average pooling is mainly because 'local block-wise distortions of different intensity' is a very local distortion type, in other words, the majority of distinctions between the original and distorted images are located in a few patches, e.g. the cyan and blue blocks in Fig. 1(e1). The global average pooling works ineffectively since it seriously decreases the influence of salient local distortions on the image quality, and thus derives an unreasonable score, as listed in Table 1.

To deal with this problem, we naturally consider the local distortion-based pooling method, which is in fact not a new issue and has been studied to some extent during the past several years. The intuitive idea of the local distortion-based pooling is to emphasize high distortion regions. Some previous work has proved its effectiveness in improving IQA prediction accuracy [16]-[17] and [26].

From another point of view, it is noted that human viewers cannot directly catch the overall information when watching an image, due to the limited sight range and processing ability of the HVS. In general, human eyes fix some salient regions before scanning the whole image. Those salient regions can be roughly regarded as the areas that are largely distinct from the surroundings. This makes those green and blue blocks in Fig. 1(e1) extremely salient relative to other areas and easy to attract the human visual attention at the first view. Broadly speaking, the first perception (e.g. the first view of an image or the first sound in a music) strongly affects the human judgements of things. This suggests that the local distortion-based pooling should be taken into consideration to tune the global average pooling for higher IQA performance.

The local distortion-based pooling is therefore applied via a simple strategy, which is defined by

$$G_l(\mathbf{x}, \mathbf{y}) = \Phi(G_s) = \frac{1}{M_s} \sum_{i=1}^{M_s} G_s(x_i, y_i) \quad (4)$$

where G_s indicates the highest $s\%$ values in G_m, and M_s is the pixel numbers in G_s. We assign s as 15 in this implementation. The G_l values of those distorted images are also evaluated and listed in Table 1. Obviously, G_l provides similar prediction scores for all of four distorted images in Fig. 1, which is quite consistent with subjective MOS val-

(a)   (b)

(c)   (d)
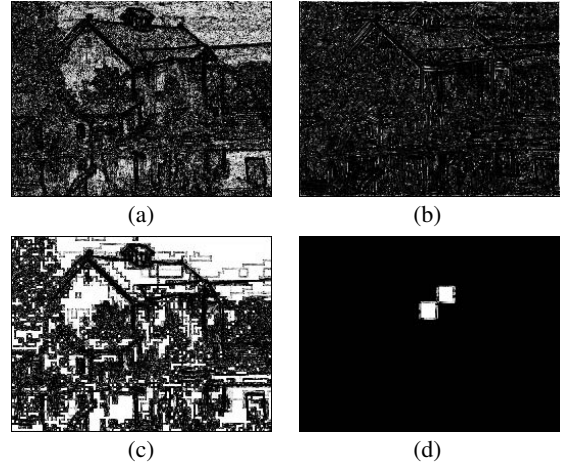
Fig. 3. Illustration of $1-G_m$ of Fig. 1(b1)-(e1). The brighter gray level means the lower similarity and higher distortion level.

ues, and thus proves the necessity of the introduction of local distortion-based pooling.

We further consider important chrominance information in this paper. Before the calculation of the GM, the simple and widely used YIQ color space [29] is adopted to transfer an input RGB color image using

$$\begin{bmatrix} Y \\ I \\ Q \end{bmatrix} = \begin{bmatrix} 0.299 & 0.587 & 0.114 \\ 0.596 & -0.274 & -0.322 \\ 0.211 & -0.523 & 0.312 \end{bmatrix} \begin{bmatrix} R \\ G \\ B \end{bmatrix} \quad (5)$$

where Y conveys the luminance information, and I and Q contain the chrominance information. In this work, we use Y to compute G_l and G_g based on Eq. (3)-(4), and use I and Q to measure the distinction of chrominance between the original and distorted images as follows:

$$I_m(\mathbf{x}, \mathbf{y}) = \frac{2I_\mathbf{x} \cdot I_\mathbf{y} + C_2}{I_\mathbf{x}^2 + I_\mathbf{y}^2 + C_2} \quad (6)$$

$$Q_m(\mathbf{x}, \mathbf{y}) = \frac{2Q_\mathbf{x} \cdot Q_\mathbf{y} + C_2}{Q_\mathbf{x}^2 + Q_\mathbf{y}^2 + C_2} \quad (7)$$

where $I_\mathbf{x}$ and $I_\mathbf{y}$ (and $Q_\mathbf{x}$ and $Q_\mathbf{y}$) represent I (Q) chromatic channels of images $\mathbf{x}$ and $\mathbf{y}$, and C_2 is similar to C_1.

Finally, the LTG is proposed to combine the above parts:

$$\text{LTG}(\mathbf{x}, \mathbf{y}) = \frac{\Phi(G_s^{\theta_1})}{\Phi(G_m^{\theta_2})} \cdot \Phi(I_m^{\theta_3} \cdot Q_m^{\theta_3}) \quad (8)$$

where θ_1 to θ_3 ($\theta_1 > \theta_2$) are model parameters. We can approximate Eq. (8) as

$$\text{LTG}(\mathbf{x}, \mathbf{y}) \approx \frac{\Phi(G_s^{\theta_1})}{\Phi(G_m^{\theta_1})} \cdot \Phi(G_m^{\theta_2'}) \cdot \Phi(I_m^{\theta_3} \cdot Q_m^{\theta_3}) \quad (9)$$

where $\theta_2' = \theta_1 - \theta_2 > 0$. The first term indicates that, for diverse images of the same G_g, the more uneven distribution of distortion levels will result in the worse quality. The second term represents the global quality. And the last term is the measure of difference in the chrominance information.

Table 2. Performance evaluations (after nonlinear regression) and the database size-weighted average of the proposed LTG and eleven competing IQA metrics on LIVE, TID2008, CSIQ, IVC, and TID2008 databases. We bold the best two performed algorithms.

Algorithms	LIVE (779 images)		TID2008 (1700 images)		CSIQ (866 images)		IVC (185 images)		TID2013 (3000 images)		Average (6530 images)	
	PLCC	SROCC	PLCC	SROCC	PLCC	SROCC	PLCC	SROCC	PLCC	SROCC	PLCC	SROCC
PSNR	0.8723	0.8756	0.5734	0.5834	0.8000	0.8033	0.7196	0.6886	0.6787	0.6875	0.6916	0.6982
SSIM	0.9449	0.9479	0.7732	0.7749	0.8613	0.8756	0.9119	0.9017	0.7895	0.7416	0.8168	0.7972
MS-SSIM	0.9489	0.9513	0.8451	0.8542	0.8991	0.9133	0.9108	0.8978	0.8329	0.7858	0.8609	0.8434
IFC	0.9268	0.9259	0.5822	0.6286	0.8390	0.7923	0.9093	0.8990	0.7218	0.6434	0.7308	0.7003
VIF	0.9603	0.9636	0.8084	0.7491	0.9264	0.9195	0.9028	0.8963	0.7719	0.6674	0.8281	0.7639
MAD	**0.9675**	**0.9669**	0.8306	0.8340	**0.9506**	**0.9467**	0.9210	0.9142	0.8271	0.8111	0.8638	0.8566
IW-SSIM	0.9522	0.9567	0.8579	0.8559	0.9144	0.9213	0.9231	0.9125	0.7638	0.7779	0.8353	0.8424
FSIM	0.9597	0.9634	0.8738	0.8805	0.9120	0.9242	0.9376	0.9263	0.8559	0.8021	0.8827	0.8615
FSIMc	**0.9613**	**0.9645**	0.8762	0.8840	0.9192	0.9310	**0.9392**	**0.9293**	**0.8768**	**0.8509**	**0.8941**	**0.8859**
GSIM	0.9512	0.9561	0.8422	0.8504	0.8964	0.9108	**0.9390**	**0.9292**	0.8463	0.7946	0.8671	0.8476
IGM	0.9567	0.9581	**0.8857**	**0.8901**	0.9281	0.9403	0.9128	0.9025	0.8561	0.8097	0.8870	0.8683
LTG	0.9534	0.9580	**0.8885**	**0.9056**	**0.9547**	**0.9603**	0.9217	0.9128	**0.8961**	**0.8819**	**0.9095**	**0.9084**

3. EXPERIMENTAL RESULTS

A comparison will be conducted in this section, to testify the performance of the proposed LTG with classical PSNR, S-SIM [12], MS-SSIM [13], IFC [14], VIF [15], and state-of-the-art MAD [18], IW-SSIM [19], FSIM [20], FSIMc [20], GSIM [21], IGM [22]. Five publicly available color image databases (LIVE [7], TID2008 [8], CSIQ [9], IVC [10], and TID2013 [11]), which have at least five distortion types, are chosen as testing beds. Referring to the suggestion given by VQEG [31], we first map the objective predictions of those twelve testing IQA metrics to subjective scores using nonlinear regression with a five-parameter logistic function:

$$Quality(q) = \gamma_1\left\{\frac{1}{2} - \frac{1}{1 + e^{(q-\gamma_3)\gamma_2}}\right\} + q\gamma_4 + \gamma_5 \quad (10)$$

with q being the input score and $Quality(q)$ the mapped s-core. The free parameters γ_1 to γ_5 are determined during the curve fitting process.

We then employ two commonly used performance evaluations, Pearson linear correlation coefficient (PLCC) and Spearman rank-order correlation coefficient (SROCC) to further measure those competing FR IQA algorithms. We report in Table 2 the performance results for each database and the database size-weighted average. It can be seen that the proposed LTG can faithfully assess image quality. Precisely, our algorithm is superior to the entire competing IQA methods on TID2008, CSIQ and TID2013, and is comparable to the state of the art on LIVE and IVC. Overall, the LTG achieves the best performance than others on average. Besides the effectiveness, we further measure the implementation speed of those IQA approaches to compare the efficiency, as tabulated in Table 3. Clearly, our technique outperforms all testing IQA metrics, except PSNR. An important note is that our LTG metric is wholly better than SSIM, which is regarded as the benchmark IQA method and embedded into most existing

Table 3. Average implementation speed (in millisecond/image).

Metrics	PSNR	SSIM	MS-SSIM	IFC
Time	**3.1223**	**38.298**	75.736	1312.7
Metrics	VIF	MAD	IW-SSIM	FSIM
Time	1167.0	1340.3	305.60	313.80
Metrics	FSIMc	GSIM	IGM	LTG
Time	326.00	70.970	9419.5	**25.313**

image/video processing systems, in the effectiveness and efficiency. Another important note is that the proposed metric is built upon the simulation of the HVS, and thus is very robust for various kinds of distortion types.

4. CONCLUSION

This paper proposes a new local-tuned-global (LTG) model to approach the process of human visual perception to image quality, and thereby introduces an efficient and effective LTG inspired color IQA algorithm. The proposed metric first extracts luminance and chrominance information from the input original and distorted RGB images. Next, we measure salient local distortions and global quality degradation in luminance information as well as compares the differences of chrominance information, thus deriving the overall image quality s-core. Experimental results on five publicly available subject-rated color image quality databases (LIVE, TID2008, CSIQ, IVC, and TID2013) are provided to confirm the effectiveness and efficiency of the proposed LTG metric over classical and state-of-the-art IQA approaches.

Acknowledgment

5. REFERENCES

[1] G. Zhai, J. Cai, W. Lin, X. Yang, and W. Zhang, "Three dimensional scalable video adaptation via user-end perceptual quality assessment," *IEEE Trans. Broadcasting*, vol. 54, no. 3, pp. 719-727, September 2008.

[2] G. Zhai, J. Cai, W. Lin, X. Yang, W. Zhang, and M. Etoh, "Cross-dimensional perceptual quality assessment for low bitrate videos," *IEEE Trans. Multimedia*, vol. 10, no. 7, pp. 1316-1324, November 2008.

[3] S. Wang, A. Rehman, Z. Wang, S. Ma, and W. Gao, "SSIM-inspired divisive normalization for perceptual video coding," *IEEE Trans. Image Process.*, vol. 22, no. 4, pp. 1418-1429, April 2013.

[4] A. Rehman and Z. Wang, "Reduced-reference image quality assessment by structural similarity estimation," *IEEE Trans. Image Process.*, vol. 21, no. 8, pp. 3378-3389, August 2012.

[5] A. Mittal, A. K. Moorthy, and A. C. Bovik, "No-reference image quality assessment in the spatial domain", *IEEE Trans. Image Process.*, pp. 4695-4708, vol. 21, no. 12, December 2012.

[6] X. Liu, D. Zhai, D. Zhao, G. Zhai, and W. Gao, "Progressive Image Denoising through Hybrid Graph Laplacian Regularization: A Unified Framework," *IEEE Trans. Image Process.*, vol. 23, no. 4, pp. 1491-1503, April 2014.

[7] H. R. Sheikh, Z. Wang, L. Cormack, and A. C. Bovik, "LIVE image quality assessment Database Release 2," [Online]. Available: http://live.ece.utexas.edu/research/quality

[8] N. Ponomarenko, V. Lukin, A. Zelensky, K. Egiazarian, M. Carli, and F. Battisti, "TID2008-A database for evaluation of full-reference visual quality assessment metrics," *Advances of Modern Radioelectronics*, vol. 10, pp. 30-45, 2009.

[9] E. C. Larson and D. M. Chandler, "Categorical image quality (CSIQ) database," [Online], Available: http://vision.okstate.edu/csiq

[10] A. Ninassi, P. Le Callet, and F. Autrusseau, "Subjective quality assessment-IVC database," [Online]. Available: http://www2.irccyn.ec-nantes.fr/ivcdb

[11] N. Ponomarenko, O. Ieremeiev, V. Lukin, K. Egiazarian, L. Jin, J. Astola, B. Vozel, K. Chehdi, M. Carli, F. Battisti, and C.-C. Jay Kuo, "Color image database TID2013: Peculiarities and preliminary results," *4th European Workshop on Visual Information Processing EUVIP2013*, pp.106-111, June 2013.

[12] Z. Wang, A. C. Bovik, H. R. Sheikh, and E. P. Simoncelli, "Image quality assessment: From error visibility to structural similarity," *IEEE Trans. Image Process.*, vol. 13, no. 4, pp. 600-612, April 2004.

[13] Z. Wang, E. P. Simoncelli, and A. C. Bovik, "Multi-scale structural similarity for image quality assessment," *IEEE Asilomar Conference on Signals, Systems and Computers*, pp. 1398-1402, November 2003.

[14] H. R. Sheikh, A. C. Bovik, and G. de Veciana, "An information fidelity criterion for image quality assessment using natural scene statistics," *IEEE Trans. Image Process.*, vol. 14, no. 12, pp. 2117-2128, December 2005.

[15] H. R. Sheikh, and A. C. Bovik, "Image information and visual quality," *IEEE Trans. Image Process.*, vol. 15, no. 2, pp. 430-444, February 2006.

[16] Z. Wang and X. Shang, "Spatial pooling strategies for perceptual image quality assessment," *Proc. IEEE Int. Conf. Image Process.*, pp. 2945-2948, October 2006.

[17] A. K. Moorthy and A. C. Bovik, "Visual importance pooling for image quality assessment," *IEEE Journal of Selected Topics in Signal Processing*, vol. 3, no. 2, pp. 193-201, April 2009.

[18] E. C. Larson and D. M. Chandler, "Most apparent distortion: Full-reference image quality assessment and the role of strategy," *Journal of Electronic Imaging*, vol. 19, no. 1, March 2010.

[19] Z. Wang and Q. Li, "Information content weighting for perceptual image quality assessment," *IEEE Trans. Image Process.*, vol. 20, no. 5, pp. 1185-1198, May 2011.

[20] L. Zhang, L. Zhang, X. Mou, and D. Zhang, "FSIM: A feature similarity index for image quality assessment," *IEEE Trans. Image Process.*, vol. 20, no. 8, pp. 2378-2386, August 2011.

[21] A. Liu, W. Lin, and M. Narwaria, "Image quality assessment based on gradient similarity," *IEEE Trans. Image Process.*, vol. 21, no. 4, pp. 1500-1512, April 2012.

[22] J. Wu, W. Lin, G. Shi, and A. Liu, "Perceptual quality metric with internal generative mechanism," *IEEE Trans. Image Process.*, vol. 22, no. 1, pp. 43-54, January 2013.

[23] K. Gu, G. Zhai, X. Yang, L. Chen, and W. Zhang, "Nonlinear additive model based saliency map weighting strategy for image quality assessment," *IEEE International Workshop on Multimedia Signal Processing*, pp. 313-318, September 2012.

[24] K. Gu, G. Zhai, X. Yang, and W. Zhang, "A new psychovisual paradigm for image quality assessment: From differentiating distortion types to discriminating quality conditions," *Signal, Image and Video Processing*, vol. 7, no. 3, pp. 423-436, May 2013.

[25] K. Gu, G. Zhai, X. Yang, and W. Zhang, "Self-adaptive scale transform for IQA metric," *Proc. IEEE Int. Symp. Circuits and Syst.*, pp. 2365-2368, May 2013.

[26] K. Gu, G. Zhai, X. Yang, W. Zhang, and M. Liu, "Structural similarity weighting for image quality assessment," *Proc. IEEE Int. Conf. Multimedia and Expo Workshops*, pp. 1-6, July 2013.

[27] K. Gu, G. Zhai, X. Yang, W. Zhang, and M. Liu, "Subjective and objective quality assessment for images with contrast change," *Proc. IEEE Int. Conf. Image Process.*, pp. 383-387, September 2013.

[28] Z. Wang and A. C. Bovik, "Mean squared error: Love it or leave it?-A new look at signal fidelity measures," *IEEE Signal Process. Mag.*, vol. 26, no. 1, pp. 98-117, January 2009.

[29] C. Yang and S. H. Kwok, "Efficient gamut clipping for color image processing using LHS and YIQ," *Optical Engineering*, vol. 42, no. 3, pp. 701-711, March 2003.

[30] B. Jähne, H. Haubecker, and P. Geibler, *Handbook of Computer Vision and Applications.* New York: Academic, 1999.

[31] VQEG, "Final report from the video quality experts group on the validation of objective models of video quality assessment," March 2000, http://www.vqeg.org/.